

PACS numbers: 42.55.Px; 41.75.Fr; 52.80.–s
DOI: 10.1070/QE2012v042n01ABEH014750

Radiation from a semiconductor target excited by an electron beam in a gas diode

K.V. Berezhnoy, M.B. Bochkarev, G.L. Danielyan, A.S. Nasibov, A.G. Reutova, S.A. Shunaylov, M.I. Yalandin

Abstract. **Radiation from a semiconductor target excited by an electron beam in a gas-filled diode was investigated at different gas (air) pressures. Subnanosecond high-voltage pulses (up to 200 kV) were applied to the pointed cathode of the diode. The targets in the form of a 15–20-μm-thick single-crystal CdS film with reflecting coatings forming an optical cavity and 0.7–1-mm-thick ZnSe plates were used. As the air pressure increased from 0.1 to 5 Torr, a decrease in the amplitude and duration of laser radiation pulses from the targets was observed. Lasing (λ = 520 nm) of CdS targets terminated at pressures greater than 2.2 Torr. The laser pulse duration varied from 125 to 20 ps. The study of the dynamics of radiation from ZnSe targets (λ = 460 nm) at atmospheric pressure showed that when the gap between the target and the electrodes was 0.2–1 mm thick, an intense near-surface glow was observed that consisted of a few pulses with the duration from 20 to 100 ps, caused by runaway electrons. Investigations showed that the runaway electrons may play an essential role in the excitation of semiconductors by subnanosecond high-voltage pulses.**

Keywords: *semiconductor laser, gas diode, runaway electrons.*

1. Introduction

When a strong electric field (10^6 – 10^7 V cm^{-1}) is applied to a semiconductor, a discharge arises and laser oscillation becomes possible. To obtain lasing one has to provide high concentration of nonequilibrium current carriers (10^{18}–10^{19} cm^{-3}) and fast switching-on of the applied field during the time, shorter than the lifetime of nonequilibrium carriers (~10^{-9} s) [1]. Such conditions are valid when the discharge develops behind the ionisation front [2–4]. Usually, a voltage pulse with the duration of tens of nanoseconds and the amplitude from 10 to 100 kV from a high-voltage pulse generator is applied through a small gap to a semiconductor sample placed in a liquid dielectric.

K.V. Berezhnoy, A.S. Nasibov P.N. Lebedev Physics Institute, Russian Academy of Sciences, Leninsky prosp. 53, 119991 Moscow, Russia; e-mail: nasibov@sci.lebede.ru, c_berezhnoy@lasertrack.ru;
G.L. Danielyan A.M. Prokhorov General Physics Institute, Russian Academy of Sciences, ul. Vavilova 38, 119991 Moscow, Russia;
M.B. Bochkarev, A.G. Reutova, S.A. Shunaylov, M.I. Yalandin Institute of Electrophysics, Ural Branch, Russian Academy of Sciences, ul. Amundsena 106, 620016 Ekaterinburg, Russia;
e-mail: yalandin@iep.uran.ru

Received 19 October 2011
Kvantovaya Elektronika **42** (1) 34–38 (2012)
Translated by V.L. Derbov

The development of high-current picosecond high-power electronics determined further progress in this direction. It was shown that the use of subnanosecond high-voltage pulses significantly improves the characteristics of an electric-discharge semiconductor laser. In particular, increasing the dielectric strength of the discharge gap allowed gap width reduction and excitation of emission in a semiconductor target (ST), paced in a gas (air)-filled diode (GFD) [5–8]. In this case the development of radiative processes in the ST is affected not only by the discharge, but also by the UV radiation and the accelerated electrons, the parameters of which are pressure-dependent. In our case, the ST is placed between the electrodes or behind the anode of the GFD designed as a coaxial chamber. The chamber is matched with a generator of high-voltage (up to 200 kV) pulses having the duration 0.3–1 ns. We study the excitation of radiation from the ST by the electron beam at different gas (air) pressures.

2. Setup

The scheme of the experimental setup is presented in Fig. 1. In the generator of high-voltage pulses (GHVP), we used the principle of front sharpening and reducing the duration of a high-voltage pulse, produced by the RADAN-3 generator, by a series connection of high-pressure discharge gaps (~10 atm) and a cutting ring slicer. To provide synchronisation with the streak camera, a high-voltage delay line is used between the last stage of the GHVP and the GFD chamber. Detailed description of the experimental setup is presented in [9, 10]. In the alternate version, the delay time is controlled by the length of fibreoptic cables [11]. The shapes and amplitudes of high-voltage pulses are fixed using capacitance dividers with the transient characteristic time ~100 ps (Fig. 1) and Tektronix TDS-6154C broad-band oscilloscope (15 GHz, sampling time 25 ps). The current in the electron beam was measured using a broad-band meter with the transient characteristic time ~70 ps.

The dynamics and pulse shape of the light pulses were studied using a streak camera with electro-optical converter [model 173, CORDIN (USA)]. To eliminate X-ray radiation and to reduce visible radiation, the lead glasses and optical filters were used. Two types of semiconductor targets were used, ST1 and ST2, made of single-crystal CdS and ZnSe, respectively. The single crystals were grown using the method of resublimation from the gas phase [12]. The target ST1 is a 15–20-μm-thick single-crystal CdS film with a reflecting coating, fixed on a sapphire disk. The target ST2 is a 0.7–1-mm-thick single-crystal ZnSe plate. The schemes of recording the radiation from the lateral and front faces of ST2 at atmospheric pressure are shown in Fig. 2.

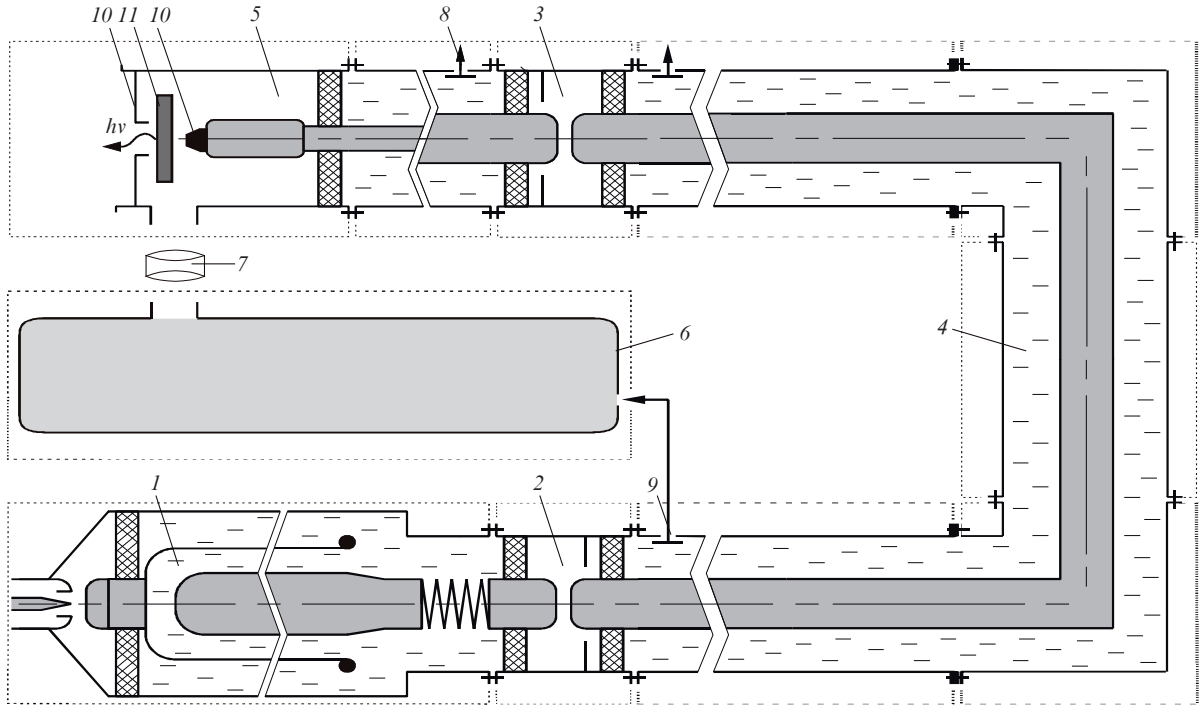

Figure 1. Setup for recording the dynamics of radiation from targets in a gas diode: (*1*) nanosecond double shaping line; (*2, 3*) subnanosecond transformers with sharpening and cutting gas discharge gaps; (*4*) high-voltage coaxial delay line; (*5*) gas diode; (*6*) streak-camera; (*7*) objective lens; (*8, 9*) capacitance voltage dividers; (*10*) electrodes of the test chamber; (*11*) semiconductor target.

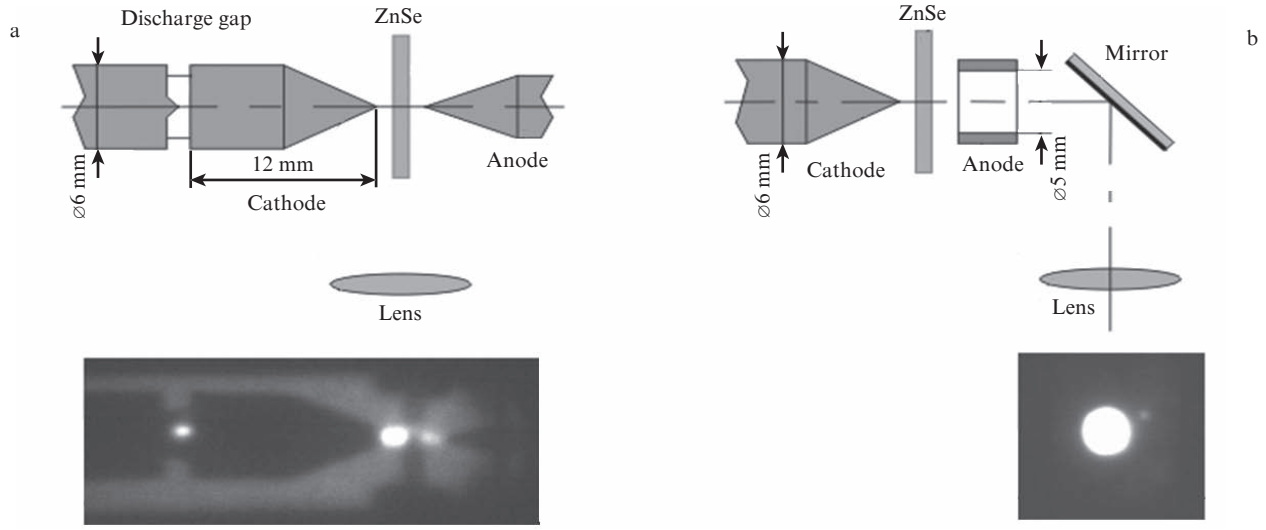

Figure 2. Scheme of recording the radiation from the lateral face (a) and from the front face (b) of the ZnSe target. The photographs of the glow are shot in the open-shutter regime without scanning and a collimating slit.

3. Experiment

The effect of the electron beam current on the parameters of radiation emitted by targets was studied at the air pressure in the GFD in the range from 10^{-1} to 5 Torr, as well as at the atmospheric pressure. In the first case, the target ST1 was mounted outside the diode, close to the diaphragm having the diameter 1 mm and covered with 15-μm-thick aluminium foil. The dependences of the electric current and ST1 radiation power pulse amplitudes on the air pressure p are presented in Fig. 3. One can seen that starting from $p \geq 1$ Torr, the pulse amplitude and duration of current and ST1 radiation decrease with increasing pressure, and the radiation power decreases faster than the amplitude of the electron beam current with increasing p. At $p > 2.2$ Torr the ST1 lasing terminated, because the current became lower than the threshold value.

Figure 4 shows streak photography of laser radiation pulses form ST1 at $p = 0.1$, 0.7, 1.5, and 2.2 Torr. The FWHM of the radiation pulse decreases from 120 to 20 ps with increasing pressure. At the pulse front in the range $p = 0.1-2$ Torr two characteristic spikes are observed. As the pressure grows, the reduction of the pulse length successively proceeds at the

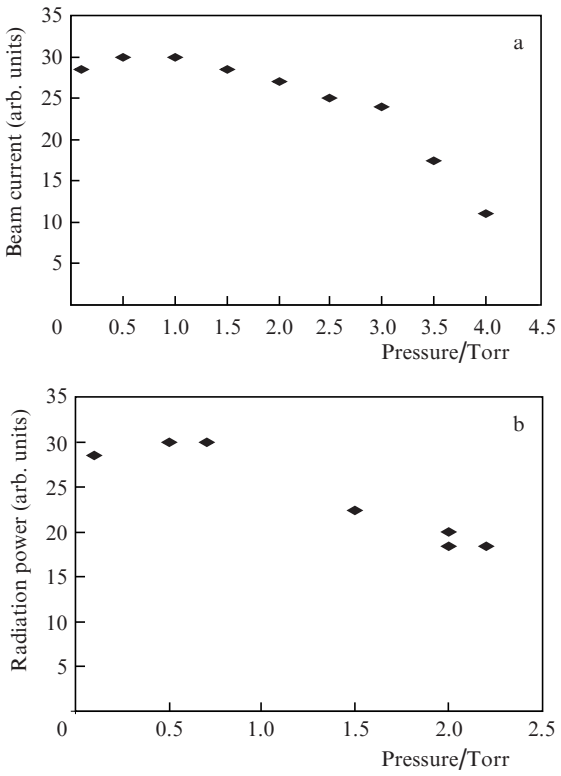

Figure 3. Dependences of the amplitudes of the electron beam current (a) and the radiation pwer (b) on the gas pressure.

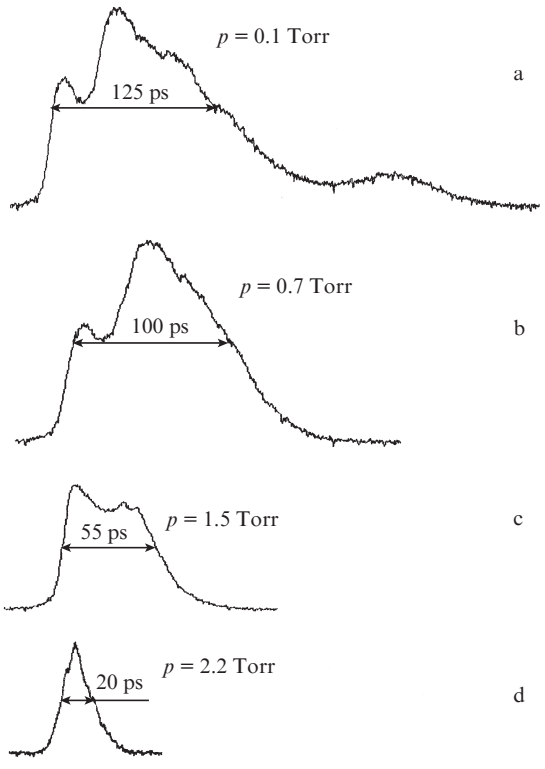

Figure 4. Change in the shape and duration of laser radiation pulses from ST1 (λ = 520 nm) excited by the electron beam at different gas pressures in the GFD.

trailing edge of the pulse, and at $p > 2$ Torr only a single spike is observed in the pulses of radiation and electron beam current.

Further studies were performed at the atmospheric air pressure. The electron current, recorded in this case, is usually referred to as the current of runaway electrons (see, e.g., [13]). A typical oscillogram of the electron current pulse at the atmospheric pressure is presented in Fig. 5. The radiation dynamics was studied in two alternate versions (Fig. 2). In the first version, the single-crystal ZnSe plate (ST2) was placed between two steel electrodes. The cathode electrode consisted of two cylinders with the diameter 6 mm, separated by a slit that served as a discharge gap. The glow of the slit discharge gap served as a reference mark for the streak-camera scanning. The conic parts of the cathode and anode electrodes had the tops with the rounding-off radius 0.5–1 mm. Such geometry of electrodes allowed maximal localisation of the radiation exit site and better recording of the radiation dynamics from the lateral face of the target (see Fig. 2a). In the second version, the anode was made in the form of a hollow steel cylinder with the inner diameter 5 mm, and the emission was recorded from the front face of ST2 (Fig. 2b). Frames of streak photography of the radiation from ST2 are presented in Fig. 6.

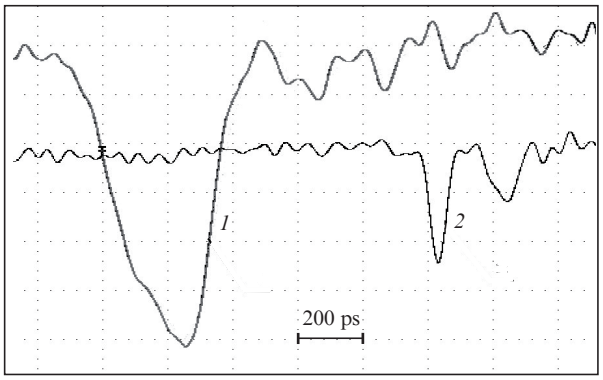

Figure 5. Typical oscillogram of a voltage pulse with amplitude 180 kV (*1*) and of the current (*2*) of runaway electrons (0.3 A) at atmospheric pressure (the tip radius of the cathode is ~1 mm, the anode is an AlBe foil).

4. Discussion

The electron beam action on semiconductor targets may be divided into two principal stages. At the first stage ($p <$ 1.5 Torr), the amplitudes of the pulses of the beam current and radiation power insignificantly change with pressure growth, whereas the pulse duration is successively reduced from the decrease side (Figs 3 and 4). The change in the beam current duration is explained by the reduction of the breakdown delay time with the pressure growth. In ST1 after attaining the threshold current density (~100 A cm^{-2}) the lasing begins. At the rising edge of the light pulses, a spike 20–40 ps long is observed.

At the second stage, starting from $p > 1.5$ Torr, the pulse amplitude and duration fastly decrease both for the beam current and for laser radiation from ST1 (Figs 3 and 4). This is explained by further reduction of the delay time and the breakdown at the front of the voltage pulse. At $p \geq 2.2$ Torr

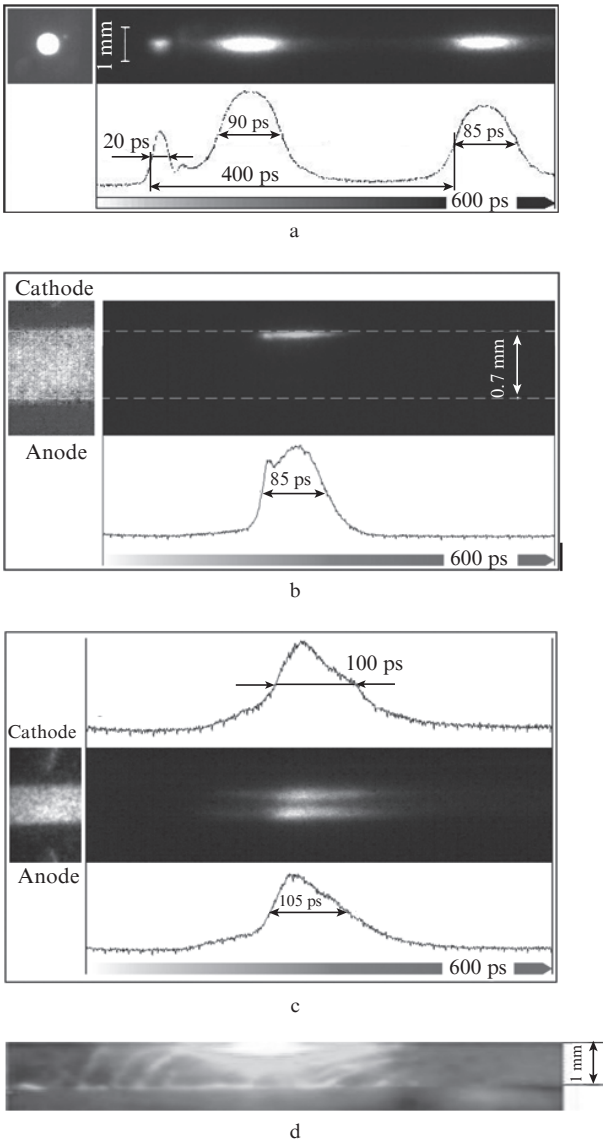

Figure 6. Streak photography of the ZnSe target radiation ($\lambda = 460$ nm) at the atmospheric pressure from the front face turned to the anode (see Fig. 2b): the cathode–plate separation is 1 mm, the plate–anode separation is 0.5 mm (a); from the lateral face (see Fig. 2a): the cathode–plate separation is 0.2 mm, the anode–plate separation is 0.75 mm (b); from the lateral face: the electrodes are 0.5 mm far from the plate (c); the photograph of the ZnSe plate glow under the action of the electron beam with the energy 170 keV (d). The depth of the near-surface excitation layer coincides with that of the glow in Fig. 6c.

(see Fig. 3b) the laser radiation from ST1 disappears, since the value of the beam current becomes lower than the threshold one.

The main results obtained for the ST2 radiation dynamics in air may be formulated as follows:

(i) the emitting region is localised near the surface (Fig. 6b) and the radiation pulse usually consists of the first spike with the duration ~20 ps and the following main (second) one with the duration 80–100 ps (Fig. 6c);

(ii) when the gap width between the cathode and the plate surface is reduced to 0.2 mm, the delay between the first short spike and the second main one is also reduced and the two spikes merge into one (Fig. 6a);

(iii) the second radiation pulse is followed by the third one, whose duration and amplitude are somewhat different (by 10%–15%) from those of the second pulse (Fig. 6a);

(iv) when the gap widths between the electrodes and the semiconductor plate surfaces are equal (0.5 mm), the emission is observed from the regions localised near both surfaces of the plate.

Let us discuss these results. When the electric discharge propagates through a semiconductor, the mean velocity of the discharge front motion usually amounts to $(3–5)\times10^8$ cm s^{-1}. During the action of the voltage pulse having the duration ~ 300 ps, the discharge front and, therefore, the emitting region of the target should move to the depth approximately equal to the thickness of the semiconductor plate (0.7–1 mm), and the duration of the light pulse, depending on the streamer length, should exceed 100 ps [2–4]. However, in our case, the emission is localised near the surface of the semiconductor and the duration of light pulses varies within the limits of 100 ps. The dependence of the time interval between the first spike and the main pulse on the separation between the cathode electrode and the plate surface is also difficult to explain.

At the same time, the phenomena observed may be well enough explained using the measurement results of the parameters of the current pulses produced by runaway electrons at atmospheric pressure (see Fig. 5). The delay time between the first spike and the main pulse of the current decreases with increasing electric field strength (equivalent to reducing the cathode-semiconductor gap width) (Figs 6a, b). The second radiation pulse corresponds to the repeated injection of electrons at the negative half-period of the voltage pulse. Figure 6d shows the photograph of the ZnSe plate emission from the lateral face. The plate was mounted directly after the vacuum-processed diode and was excited by a beam of electrons with the energy 170 keV and the current density ~100 A cm^{-2}. The similarity of the near-surface glow of the plates in Fig. 6d and Fig. 6c is apparent, which confirms the hypothesis that the glow of the plates under the atmospheric pressure arises under the action of the beam of runaway electrons. After the end of the current pulses, the diode conductance abruptly increases (the breakdown occurs), which usually gives rise to a streamer discharge in the semiconductor. The absence of the discharge channels connecting one plane of the target with the other is explained by the bypass effect of the target surface, since the target conductance increases under the action of the ionising radiation.

Nevertheless, a number of questions hard to answer still exist. One of them relates to the origin of intense near-surface radiation, usually observed at a high enough beam current density. Indeed, the threshold current density, at which superluminescence and lasing arise in II–VI semiconductor lasers at accelerating voltages 100–200 kV and room temperature usually amounts to ~100 A cm^{-2} [9]. Meanwhile, the current density of the electron beam, obtained earlier in the experiments with a gas-filled diode at atmospheric pressure, did not exceed a few A cm^{-2} [14, 15]. It should be noted also that the electrodes geometry and interelectrode separations in [14, 15] were strongly different from ours and typically implied sleeve cathodes up to 6 mm in diameter with the cathode–anode separation varying within 5–10 mm. In our case, two conical electrodes were separated by a 0.2–0.75-mm gap from the high-resistance (~10^8 Ω cm) 1-mm-thick plate with static dielectric constant $\varepsilon \sim 8$, which provided significant strengthening and concentration of the electric field in the gaps

between the plate and the electrodes. Since the diameter of the light-emitting spot amounted to 100–200 μm (Fig. 6a), even at small beam currents (no greater than 0.1 A), the current density could strongly exceed the threshold value (~100 A cm^{-2}). Streak photography in the case of equidistant electrodes (Fig. 6c) shows that the emission from the opposite sides of the plate is synchronous and occurs during the negative half-period of the voltage pulse. Otherwise the radiation pulse from the anode side of the plate would be shifted in time with respect to the pulse from the opposite side. The explanation of synchronous emission from both sides may be given as follows. The electron beam from the cathode side excites the target and changes the polarity of this side of the plate to negative. In response, the polarity of the anode side of the plate changes to positive, causing electron beam injection and plate emission excitation.

The origin of sequential light pulses (Fig. 6a) is due to the fact that the first pulse (with the 20-ps duration) is produced by a cluster of runaway electrons acting on the target, while the second (90 ps) and the third (85 ps) pulses correspond to the current oscillations, related to negative half-periods of the voltage oscillations.

The studies have shown that upon excitation of radiation from semiconductor targets by subnanosecond high-voltage pulses [5–8], it is necessary to take into account the influence of the electron beam, arising in the gas medium in the broad range of pressure values.

Acknowledgements. The work was supported by the Russian Foundation for Basic Research (Grant Nos 09-08-00371-a and 10-08001219-a).

References

1. Basov N.G., Vul B.M., Popov Yu.M. *Zh. Eksp. Teor. Fiz*., **37**, 587 (1959) [*Sov. Phys. JETP*, **10**, 416 (1960)].
2. Basov N.G., Molchanov A.G., Nasibov A.S., Obidin A.Z., Pechenov A.N., Popov U.M. *IEEE J. Quantum Electron.*, **10** (9), 794 (1974).
3. Basov N.G., Molchanov A.G., Nasibov A.S., Obidin A.Z., Pechenov A.H., Popov Yu.M. *Zh. Eksp. Teor. Fiz.*, **70** (5), 1750 (1976) [*Sov. Phys. JETP*, **43**, 912 (1976)].
4. Nasibov A.S., Obidin A.Z., Pechenov A.N., Popov Yu.M., Frolov V.A. *Pis'ma Zh. Tekh. Fiz*., **5** (1), 22 (1979) [*Sov. Tech. Phys. Lett*., **5**, 9 (1979)].
5. Mesyats G.A., Nasibov A.S., Shpak V.G., Shunaylov S.A., Yalandin M.I. *Zh. Eksp. Teor. Fiz.*, **133** (6), 1162 (2008). [*JETP*, **106** (6), 1013 (2008)].
6. Mesyats G.A., Nasibov A.S., Shpak V.G., Shunaylov S.A., Yalandin M.I. *Kvantovaya Elektron*., **38** (3), 213 (2008) [*Quantum Electron*., **38** (3), 213 (2008)].
7. Berezhnoy K.V., Nasibov A.S., Shapkin P.V., Spak V.G., Sunaylov S.A., Yalandin M.I. *Kvantovaya Elektron.*, **38** (9), 829 (2008) [*Quantum Electron*., **38** (9), 829 (2008)].
8. Berezhnoy K.V., Nasibov A.S., Reutova A.G., Shapkin P.V., Shunailov S.A., Yalandin M.I. *Optical Memory and Neural Networks (Information Optics)*, **18** (4), 285 (2009).
9. Nasibov A.S., Berezhnoy K.V., Shapkin P.V., Reutova A.G., Shunaylov S.A., Yalandin M.I. *Prib. Tekh. Eksp*., (1), 75 (2009) [*Instrum. Exp. Tech*., **52**, 65 (2009)].
10. Berezhnoy K.V., Bochkarev M.B., Nasibov A.S., Reutova A.G., Shunaylov S.A., Yalandin M.I. *Prib. Tekh. Eksp*., (2), 124 (2010) [*Instrum. Exp. Tech*., **53**, 272 (2010)].
11. Nasibov A.S., Berezhnoy K.V., Bochkarev M.B., Danielyan G.L., Reutova A.G., Shunaylov S.A., Yalandin M.I. *Sb. dokl. 20 Mezhd. konf. 'Lazery, izmereniya, informatsiya'* (Proc. Int. Conf. 'Lasers, Measurements, Information') (Saint-Petersburg, SSPU Publishers, 2010) Vol. 1, pp 5–13.
12. Korostelin Yu.V., Tikhonov V.G., Shapkin P.V. *Trudy FIAN*, **202**, 202 (1991).
13. Korolev Yu.D., Mesyats G.A. *Fizika impul'snogo prboya gazov* (Physics of Pulsed Breakdown in Gases) (Moscow: Nauka, 1991).
14. Mesyats G.A., Korovin S.D., Sharypov K.A., Shpak V.G., Shunaylov S.A., Yalandin M.I. *Pis'ma Zh. Tekh. Fiz*., **32** (1), 35 (2006) [*Tech. Phys. Lett.*, **32**, 18 (2006)].
15. Tarasenko B.F., Rybka D.V., Baksht E.Kh., Kostyrya I.D., Lomaev M.I. *Prib. Tekh. Eksp*., (2), 62 (2008) [*Instr. Exp. Tech.*, **51**, 213 (2008)].